IFSCC 2025 full paper IFSCC2025-1019

miRNA408 from Camellia japonica L. mediates cross-kingdom regulation in human skin recovery

Jae-Goo Kim[1], Hye Jin Kim[1], Ji Young Kim[1], Soll Jin[1], Hee Cheol Kang[1,] * and Mi Jung Kim[1,] *

[1] Human & Microbiome Communicating Laboratory, GFC Co., Ltd., Hwaseong 18471, Republic of Korea; * Correspondence: mj2.kim@gfcos.co.kr (M.J.K.), michael@gfcos.co.kr (H.C.K.)

1. Introduction

In recent years, interest in plant-derived substances as potentialtherapeutic agents has been growing, particularly extracellular vesicles (EVs) [1]. Furthermore, exosomes, a subtype of EVs, have gained owing to their ability to mediate intercellular communication by transferring various bioactive molecules. They possess a stable structure characterized by a phospholipid bilayer and play a crucial role in cellular signaling [2]. Recent studies have highlighted the therapeutic potential of plant-derived vesicles (PDVs).

miRNAs are short non-coding RNA molecules that play a critical role in regulating gene expression by interacting with messenger RNA (mRNA). By binding to the target mRNA, miRNAs inhibit gene translation or destabilize the mRNA, thereby modulating protein expression levels [3]. Their altered expression patterns, which often change in response to disease conditions, make them promising diagnostic and prognostic tools for biomedical research. Since the potential of microRNAs(miRNAs or miRs) as biomarkers was first recognized, miRNAs have been extensively studied and cited in the literature for their potential application as biomarkers of diseases.

This study aimed to explore the therapeutic potential of these plant-derived miRNAs from EVs for skin health applications in skin health. Understanding the interactions between plant-derived miR408 from EVs and human skin cells may offer novel insights into the molecular pathways associated with skin aging [4]. The discovery of cross-kingdom regulatory mechanisms mediated by miR408 may pave the way for therapeutic applications and innovative skincare strategies that utilize plant-derived miRNAs from EVs [5].

2. Materials and Methods

Callus induction of *Camellia japonica* L. and suspension culture

For induction of callus from leaves of *C. japonica* L. (Cj-callus), leaves were sterilized by soaking in ethanol, followed by treatment with a disinfectant solution. The sterilized leaves were washed with sterile distilled water, supplemented with cefotaxime sodium. The leaves were cut and placed on an Murashige and Skoog medium. The cultures were maintained in the dark to promote callus formation. Subsequently, the callus was transferred to liquid medium and cultured under suspension conditions.

Isolation of extracellular vesicles (EVs) from *C. japonica* L.

EVs from *C. japonica* callus (Cj-callus EVs) were isolated using a liquid suspension culture system. Four-week-old Cj-callus cultures from a bioreactor were first separated into callus

clusters and conditioned medium using mesh filters. The medium was then centrifuged and only the supernatant was collected. The cleared supernatant was further subjected to ultracentrifugation. The supernatants were carefully discarded, and the EV pellet was resuspended in a small volume of deionized water. The EV suspension was filtered through a 0.22 μm syringe filter for sterilization and stored at -80 ℃ until further use. Nanoparticle imaging was conducted using a transmission electron microscope. EVs were placed onto carbon-coated grids. The grids were then stained with 2% uranyl acetate solution.

Western blot analysis

Equal amounts of protein were separated on SDS-polyacrylamide gels and transferred onto polyvinylidene fluoride membranes. Transferred membranes were blocked and then incubated with primary antibodies: anti-TET8 or anti-PEN1. Following washing with TBST, membranes were incubated with HRP-conjugated secondary antibody. The membranes were developed on a chemiluminescence imaging system.

Cell culture

The human keratinocyte (HaCaT) and human fibroblast (HFF) cell line were cultured in Dulbecco's modified Eagle medium, supplemented with 10% fetal bovine serum and 1% of a penicillin–streptomycin solution. Cells were maintained at 37 ℃ with 5% CO_2.

Cell viability assay

Cultured cells were treated with EVs at specified concentrations or transfected with a microRNA mimic for each experiment and incubated. Cell viability was assessed using WST-1 cell proliferation and cytotoxicity detection kit following the manufacturer's protocol. The absorbance was then measured at 450 nm.

Extracellular vesicles uptake assay

EVs were labeled with LipidyeII according to the manufacturer's protocol. Hoechst 33342 was applied to cultured cells for nuclear counterstaining and subsequently add the labeled EVs to each well. After treatment, the wells were washed, and cells were fixed in 4% paraformaldehyde. Fluorescence images were obtained using a fluorescence microscope.

***In vitro* wound healing assay**

The cells were seeded using Wound Healing Insert. Following incubation, the inserts were carefully removed, and the wells were washed. The cells were then treated with EVs at an optimized concentration in a serum-free medium for an additional 48 hours. The size of the cell-free gaps was visualized detected under a microscope and measured using Image J.

Immunocytochemistry (ICC)

Following UVA exposure, cells were either treated with EVs or transfected with a microRNA mimic, as specified for each experimental condition, and then incubated for an additional 48 hours. After incubation, supernatants were discarded, and the cells were gently washed before fixation in 4% paraformaldehyde. Fixed cells were washed, permeabilized with 0.1% Triton- X 100 and washed again. Subsequently, a 5% bovine serum albumin blocked the cells and then the cells were incubated with collagen type I A1. The cells were incubated with the conjugated Alexa Fluor 488 for secondary antibody, followed by and staining with DAPI. Finally, the cell images were taken using a fluorescence microscope.

ELISA

Following initial culture, the medium was replaced with a fresh medium containing EVs or miRNA mimics at varying concentrations, and cells were incubated for an additional 24 hours. After incubation, supernatants were collected and centrifuged. IL-6 expression levels in the supernatants were quantified using a human IL-6 ELISA kit according to the manufacturer's instructions. Absorbance was measured at 450 nm to determine IL-6 concentrations.

qRT-PCR (Quantitative reverse-transcription PCR)

After incubation, cells were then treated with appropriately diluted EVs and incubated for another 24 hours. Total RNA was isolated using the NucleoSpin RNA kit according to the manufacturer's instructions, and RNA quantity was assessed. cDNA was synthesized using a cDNA synthesis kit. Target gene expression was detected with SYBR Green Supermix. Expressions levels were normalized to β-actin as an internal control, and relative gene expression was calculated using the $2^{-\triangle\triangle Ct}$ method.

Small RNA isolation

Small RNA was isolated from Cj-callus and Cj-callus EVs using a XENOPURE Plant Small RNA Purification kit and XENO-EVARI Kit, respectively, following the manufacture's instruction. Purified RNA samples were further cleaned using the XENOPURE Small RNA clean-up kit, as instructed. All RNA samples were stored at -80 ℃ until subsequent analysis.

Small RNA Library construction and analysis

Small RNA libraries were generated using the XENO-LIBERA library kit according to the manufacturer's instructions. Sequencing was conducted on an Illumina NextSeq 500 platforms. The quality of raw miRNA-seq data was performed using FastQC v0.11.9 [6], and adaptor sequences were removed using Cutadapt v4.4 [7]. Only reads of 18-30 nucleotides were retained, and the 3′ bases with a quality score below 20 were trimmed. Trimmed data were further processed to collect reads aligned with non-coding RNA sequences using Bowtie v1.1.2 [8]. miRNA prediction was conducted using the miRkwood tool [9] alongside BrumiR v3.0 [10]. To quantify miRNA expression levels, clean miRNA-seq reads were mapped to the predicted miRNAs, which were subsequently compared against the miRBase database [11] for validation. Predicted miRNA families were further identified using BLASTn v2.2.29 in the NCBI-BLAST package [12].

3. Results

Isolation and Characterization of the EVs from the callus of *C. japonica* L.

The biophysical properties of Cj-callus EVs were assessed by measuring their size, particle concentration, and zeta potential using nanoparticle tracking analysis (Fig. 1a). Transmission electron microscopy revealed the shape and size characteristics of Cj-callus EVs (Fig. 1b). Western blot analysis was conducted to assess the expression of TET8 and PEN1, which are well-known biomarkers of plant-derived extracellular vesicles from *Arabidopsis thaliana* (Fig. 1c) [13. 14].

Enhanced Wound Healing Activity by Cj-callus EVs in Skin Cells

To evaluate the biological efficacy of Cj-callus EVs, cell viability assays were. The results showed no significant differences in cell viability, regardless of the EV concentration (Not shown). Fluorescently labeled EVs were observed within the cytoplasm indicating successful uptake and the potential for cross-kingdom interactions (Fig. 2a). To explore the wound-healing potential of Cj-callus EVs, Cj-callus Evs treated HFFs significantly accelerated wound closure in a dose-dependent manner(Fig. 2b). To determine the effects of Cj-callus EVs on damage repair in UVA-exposed fibroblasts, immunocytochemistry and qRT-PCR were performed. *COL1A1* and *COL1A2* expression was significantly upregulated in Cj-callus EV-treated cells, with increases of 4.31 and 3.24-fold, respectively. *MMP1* expression was downregulated by 39.29%, similar to the positive controls (Fig. 2c). Collagen expression in HFF decreased following UVA exposure; however, treatment with Cj-callus EVs restored type I collagen expression (Fig. 3d).

a

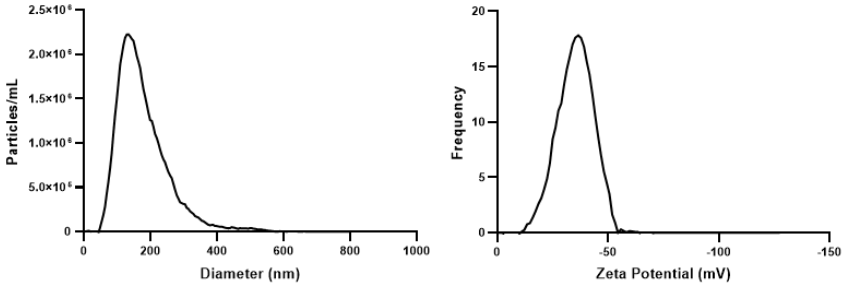

Concentration (particle/mL)	Size (nm)	Zeta-potential (mV)
1.3 X 10^{10}	155.8	-35.34

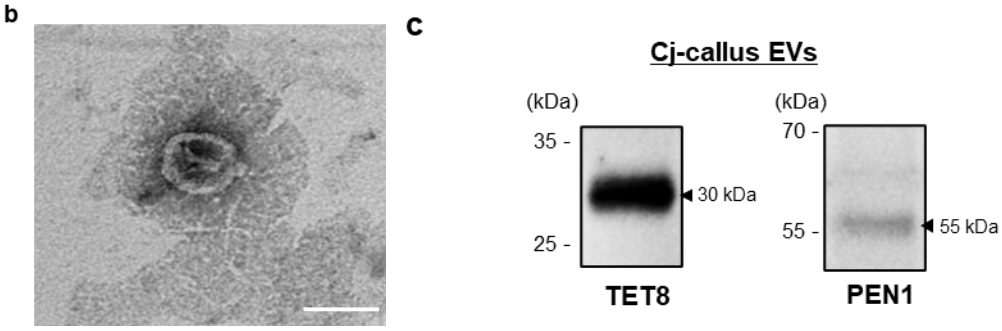

Figure 1. Characterization of Cj-callus Evs
(a) Resutls from NTA of Cj-callus EVs, detailing the size, concentration, and zeta-potential. (b) An image of Cj-callus EVs was captured by transmission electron microscopy. Scale bar, 100 nm. (c) Western blot result of Cj-callus EVs.

Anti-inflammatory Activity by Cj-callus EVs in keratinocyte

To evaluate the anti-inflammatory activity of Cj-callus EVs in human keratinocytes (HaCaT), we measured changes in IL-6 production following treatment with Cj-callus Evs. Treatment with EVs resulted in a 68.21% reduction in *IL6* gene expression (Fig. 3a). Furthermore, IL-6 protein production decreased by 57.20% in Cj-callus EV-treated under the same inflammatory conditions (Fig. 4b).

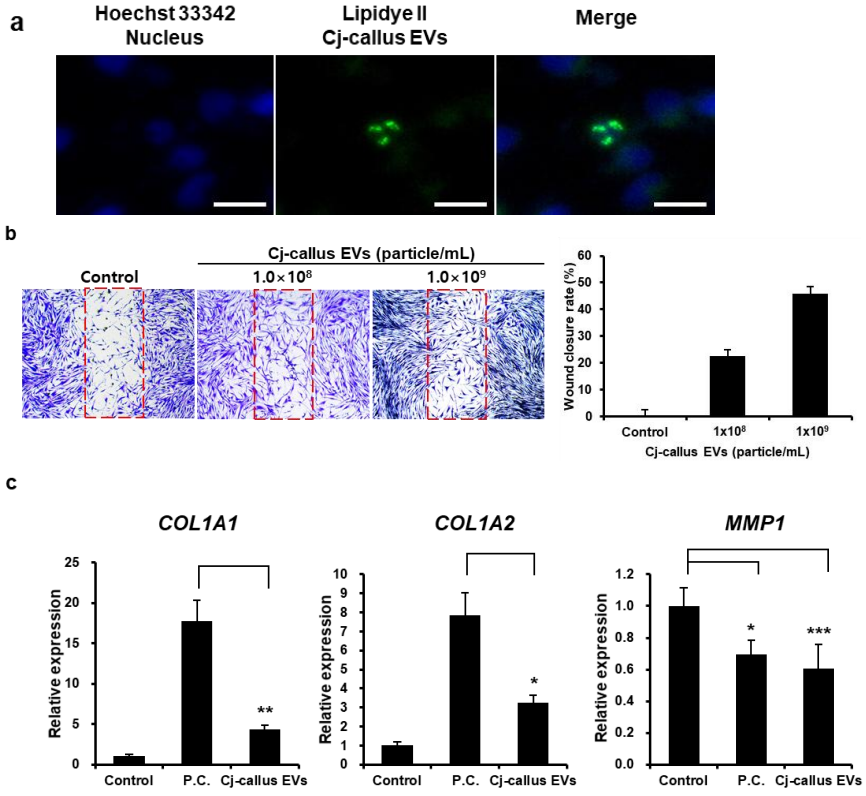

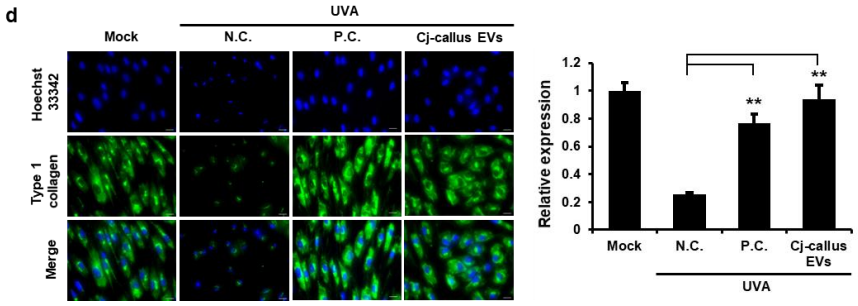

Figure 3. EVs uptake assay and Wound healing by Cj-callus EVs
(a) Stained EVs' uptake by keratinocyte. Scale bar, 10 μm. (b) Images of wound healing activity by EVs in fibroblast, along with a graph showing the rate of wound closure after EV treatment. Red dotted line indicates the wound area. (c) qRT-PCR results of collagen and MMP gene expression after UVA exposure. *p < 0.05; **p < 0.01, ***p < 0.001. (d) N.C., Negative control, P.C., Scale bar, 20 μm. **p < 0.01.

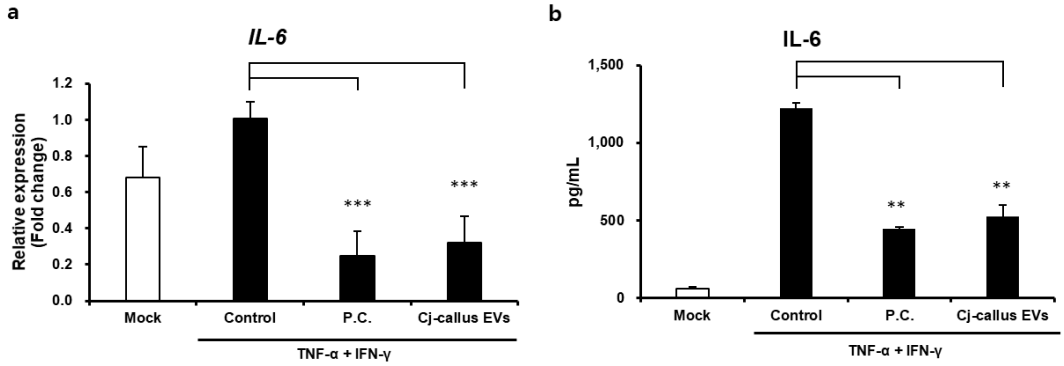

Figure 4. Anti-inflammatory activity of EVs derived from *C. japonica* L.
(a) Relative expression level of IL-6 mRNA with EVs. P.C., 10 ng/mL TGF-β; ***p < 0.001. (b) IL-6 protein expression are down-regulated with EVs. **p < 0.01.

Enrichment of miR408 in Cj-callus EVs

To identify and characterize the miRNAs in Cj-callus EVs, small RNA sequencing was performed on both Cj-callus and Cj-callus EVs derived from the induced calli. This approach enabled the identification and quantification of individual miRNAs. After trimming the reads to 20–30 nucleotides, the composition of the small RNA categories within the trimmed callus and the EV reads was shown in Table 1. Notably, the miRNA content in EVs was approximately 1.62 times higher than that in calli, suggesting that EVs selectively enrich and concentrate miRNAs. Although the overall composition ratios of small RNA were similar between the two groups, miRNAs were significantly more abundant in EVs, both in terms of proportion and read count. Further analysis identified eight distinct miRNA families enriched in Cj-callus Evs (Fig. 5). These findings highlight the selective enrichment of miRNAs, particularly miR408, suggesting a potential regulatory role of EV-associated miRNAs in various biological functions.

Table 1. Composition of small RNA from Cj-callus and Cj-callus Evs

		Trimmed reads	miRNA	rRNA	tRNA	CDS	ncRNA
Cj-callus	#	20,070,253	8,233	3,779,905	31,977	4,098,468	12,151,670
	%	100	0.04	18.83	0.16	20.42	60.55
Cj-callus EVs	#	3,101,319	13,351	316,953	22,523	1,013,805	1,734,687
	%	100	0.43	10.22	0.73	32.69	55.93

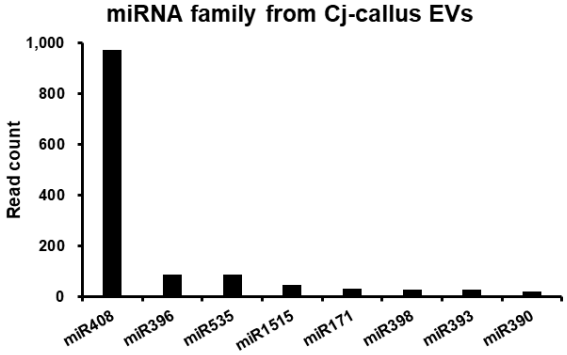

Figure 5. Small RNA sequencing of callus and EVs derived from *C. japonica* L.
miRNA list from Cj-callus EVs according to read counts. The E-value is a corrected bit-score adjusted to the sequence database size.

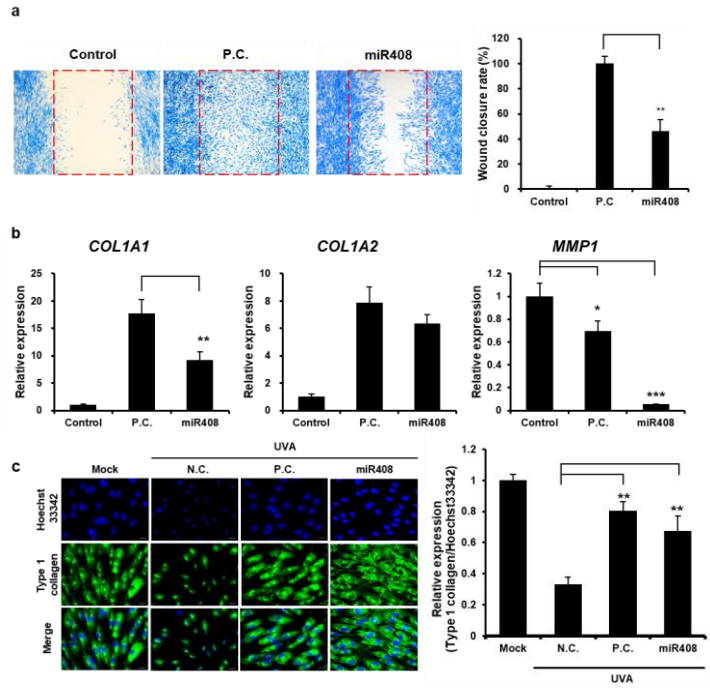

Figure 6. In vitro wound healing activity of miR408 from Cj-callus EVs
(a) Images depicting the wound healing activity of miR408 in fibroblasts. Red dotted line indicates the wound area. **p < 0.01. (b) qRT-PCR results of collagen and MMP gene expression after UVA exposure. P.C., 10 ng/mL TGF-β. *p < 0.05; **p < 0.01, ***p < 0.001. (c) miR408 restores type I collagen in fibroblasts following UVA exposure; Scale bar, 20 μm. **p < 0.01

Bioactivity of miR408 in Cj-callus EVs

To determine whether EV-derived microRNAs have bioactivity similar to that of EVs, miR408, the most abundant miRNA in EVs, was selected for further investigation. There were no significant differences in cell viability by miR408 (Not shown). However, miR408 increased the wound closure rates in fibroblasts by 46.19% compared to the control (Fig. 6a). To evaluate the impact of miR408 on the repair of UVA-induced damage in fibroblasts, immunocytochemistry and qRT-PCR were performed to evaluate collagen and *MMP1* expression.The results showed significant upregulation of *COL1A1* and *COL1A2* expression following miR408 treatment, with increases of 9.17-fold and 6.38-fold, respectively. Additionally, *MMP1* expression was markedly downregulated by 99.95%, demonstrating a much stronger inhibition than that of the positive control (Fig. 6b). After treatment with miR408 at, type I collagen expression recovered, showing a 34.27% increase (Fig. 6c).

In HaCaT cells, treatment with miR408 at a 10 nM concentration resulted in a 68.21% reduction in *IL6* gene expression (Fig. 7a). Additionally, IL-6 protein production decreased by 57.20% in miR408 treated HaCaT cells under the same inflammatory conditions (Fig. 7b).

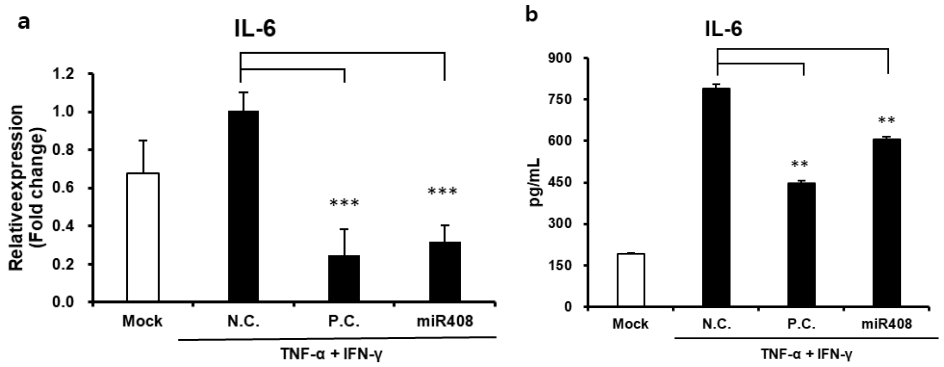

Figure 7. Anti-inflammatory activity of miR408 from EVs
(a) miR408 decrease the gene expression of IL-6. P.C., 10 ng/mL TGF-β; ***p < 0.001. (b) IL-6 protein level is reduced with miR408 treatment. **p < 0.01..

4. Discussion

Camellia japonica L., commonly known as Japanese camellia or Tsubaki, is highly valued in the cosmetic industry because of its beneficial effects on skin health. The oil extracted from camellia seeds is known for its exceptional moisturizing, hydrating, and skin-nourishing properties [15]. Our results highlight the potential of Cj-callus EVs in various sectors, particularly cosmetics, pharmaceuticals, and agriculture, contributing to the expanding research landscape of plant-derived EVs and their diverse applications.

Our findings also revealed that Cj-callus EVs exhibited notable wound healing and anti-inflammatory effects. In fibroblast cell viability and wound closure assays, treatment with increasing concentrations of Cj-callus EVs resulted in enhanced wound closure, indicating their ability to accelerate healing. This outcome aligns with previous research suggesting that EVs carry bioactive molecules that can promote cell migration, proliferation, and extracellular matrix remodeling during wound healing processes [16]. Notably, the reduction in IL-6, a cytokine closely associated with inflammation, aging, and skin damage, highlighted the protective role of Cj-callus EVs in managing inflammatory skin conditions. These findings suggest that Cj-callus EVs could serve as promising agents for therapeutic applications targeting skin inflammation, wound healing, and aging.

Plant miRNAs play a crucial role in plant development and growth, particularly in regulating processes. Research in 2012 discovered that plant-derived miRNAs regulate gene expression in mammals, which sparked significant interest in cross-kingdom miRNA interactions [17]. Our findings highlight the impact of miR408 as a novel bioactive role that extends across species. miR408, identified in plants, is known for its significant physiological functions across various plant species. Predominantly expressed in chloroplasts, miR408 regulates several key processes, including photosynthesis and chlorophyll biosynthesis [18]. These attributes have made exploring the potential effects of miR408 beyond plant biology an emerging area of interest. miR408 independently enhanced wound healing by promoting wound closure, similar to the effects observed with Cj-callus EVs and restored COL1A1 expression to higher levels, with a significant reduction in MMP1 expression. Additionally, miR408 exhibits notable anti-inflammatory properties by decreasing IL-6 expression in human keratinocytes. These results indicate that miR408 plays a crucial role in the wound healing and anti-inflammatory activities of Cj-callus EVs, likely through cross-kingdom regulatory mechanisms. However, further research is required to explore the correlation between these genes, wound closure, and their anti-inflammatory effects.

5. Conclusion

Overall, this study suggests that Cj-callus EVs enriched with functional miR408 have significant therapeutic potential for dermatological applications, particularly in wound healing and

inflammation modulation. Future research should focus on elucidating the mechanisms of EV uptake in human skin cells, exploring the pathways modulated by miR408, and assessing the potential of Cj-callus EVs *in vivo*. This study provides a foundation for the development of plant-derived EV-based formulations and emphasizes the therapeutic relevance of plant-derived EVs in skin health and anti-aging applications.

6. References

[1] Rome S. Biological properties of plant-derived extracellular vesicles. Food. Funct. 10, 529–538. (2019).

[2] Zhang, H., et al. Identification of distinct nanoparticles and subsets of extracellular vesicles by asymmetric flow field-flow fractionation. Nat. Cell. Biol. 20, 332–343 (2018).

[3] Millar A. A. The Function of miRNAs in Plants. Plants 9, 198 (2020).

[4] Xiao, J., et al. Identification of exosome-like nanoparticle-derived microRNAs from 11 edible fruits and vegetables. PeerJ 6, e5186 (2018).

[5] Horsburgh, S., et al. MicroRNAs in the skin: role in development, homoeostasis and regeneration. Clin. Sci. 131, 1923–1940 (2017).

[6] Martin, M. Cutadapt removes adapter sequences from high-throughput sequencing reads. EMBnet. J. 17, 10-12 (2011).

[7] Langmead, B., et al. Ultrafast and memory-efficient alignment of short DNA sequences to the human genome. Genome. Biol. 10, R25 (2009).

[8] Guigon, I., et al. miRkwood: a tool for the reliable identification of microRNAs in plant genomes. BMC. Genomics. 20, 532 (2019).

[9] Moraga, C., et al. BrumiR: A toolkit for de novo discovery of microRNAs from sRNA-seq data. GigaScience. 11, giac093 (2022).

[10] Gbriffiths-Jones, S., et al. miRBase: microRNA sequences, targets and gene nomenclature. Nucleic. Acids. Res. 34, D140-144 (2006).

[11] Camacho, C., et al. BLAST+: architecture and applications. BMC Bioinform. 10, 421 (2009).

[12] He, B., et al. RNA-binding proteins contribute to small RNA loading in plant extracellular vesicles. Nat. Plants. 7, 342–352 (2021).

[13] Rutter, B. D., and Innes, R. W. Extracellular Vesicles Isolated from the Leaf Apoplast Carry Stress-Response Proteins. Plant. Physiol. 173, 728–741 (2017).

[14] Jung, E., et al. Effect of Camellia japonica oil on human type I procollagen production and skin barrier function. J.Ethnopharmacol. 112, 127–131 (2007).

[15] Efferth, T. Biotechnology applications of plant callus cultures. Eng. 5, 50-59 (2019).

[16] Narauskaitė, D., et al. xtracellular Vesicles in Skin Wound Healing. Pharm. 14, 811 (2021).

[17] Zhang, L., et al. Exogenous plant MIR168a specifically targets mammalian LDLRAP1: evidence of cross-kingdom regulation by microRNA. Cell. Res. 22, 107–126 (2012).

[18] Gao, C., et al. Co-occurrence networks reveal more complexity than community composition in resistance and resilience of microbial communities. Nat. Commun. 13, 3867 (2022).